Match-up database Analyses Report

SMAP-L3-RSS-V3-8DAY-RUNNING-70KM

Argo

Congo river plume

prepared by the Pi-MEP Consortium

March 15, 2019

Contents

List of Figures

Acronym

Aquarius	NASA/CONAE Salinity mission
ASCAT	Advanced Scatterometer
ATBD	Algorithm Theoretical Baseline Document
BLT	Barrier Layer Thickness
CMORPH	CPC MORPHing technique
CTD	Instrument used to measure the conductivity, temperature, and pressure of seawater
DM	Delayed Mode
EO	Earth Observation
ESA	European Space Agency
FTP	File Transfer Protocol
GOSUD	Global Ocean Surface Underway Data
GTMBA	The Global Tropical Moored Buoy Array
Ifremer	Institut français de recherche pour l'exploitation de la mer
IPEV	Institut polaire français Paul-Émile Victor
IQR	Interquartile range
ISAS	In Situ Analysis System
Kurt	Kurtosis (fourth central moment divided by fourth power of the standard deviation)
L2	Level 2
LEGOS	Laboratoire d'Etudes en Géophysique et Océanographie Spatiales
LOCEAN	Laboratoire d'Océanographie et du Climat : Expérimentations et Approches Numériques
LOPS	Laboratoire d'Océanographie Physique et Spatiale
MDB	Match-up Data Base
MEOP	Marine Mammals Exploring the Oceans Pole to Pole
MLD	Mixed Layer Depth
NCEI	National Centers for Environmental Information
NRT	Near Real Time
NTAS	Northwest Tropical Atlantic Station
OI	Optimal interpolation
Pi-MEP	Pilot Mission Exploitation Platform
PIRATA	Prediction and Researched Moored Array in the Atlantic
QC	Quality control
R_{sat}	Spatial resolution of the satellite SSS product
RAMA	Research Moored Array for African-Asian-Australian Monsoon Analysis and Prediction
r^2	Square of the Pearson correlation coefficient
RMS	Root mean square
RR	Rain rate
SAMOS	Shipboard Automated Meteorological and Oceanographic System
Skew	Skewness (third central moment divided by the cube of the standard deviation)
SMAP	Soil Moisture Active Passive (NASA mission)
SMOS	Soil Moisture and Ocean Salinity (ESA mission)
SPURS	Salinity Processes in the Upper Ocean Regional Study
SSS	Sea Surface Salinity
SSS_{insitu}	In situ SSS data considered for the match-up

SSS_{SAT}	Satellite SSS product considered for the match-up
ΔSSS	Difference between satellite and in situ SSS at colocalized point ($\Delta SSS = SSS_{SAT}$- SSS_{insitu})
SST	Sea Surface Temperature
Std	Standard deviation
Std*	Robust Standard deviation = median(abs(x-median (x)))/0.67 (less affected by outliers than Std)
Stratus	Surface buoy located in the eastern tropical Pacific
Survostral	SURVeillance de l'Océan AuSTRAL (Monitoring the Southern Ocean)
TAO	Tropical Atmosphere Ocean
TSG	ThermoSalinoGraph
WHOI	Woods Hole Oceanographic Institution
WHOTS	WHOI Hawaii Ocean Time-series Station
WOA	World Ocean Atlas

1 Overview

In this report, we present systematic analyses of the Match-up DataBase (MDB) files generated by the Pi-MEP platform within the following Pi-MEP region and for the below pair of Satellite/In situ SSS data:

- Pi-MEP region: Congo river plume (download the corresponding mask here)

- SSS satellite product (SSS_{SAT}): SMAP-L3-RSS-V3-8DAY-RUNNING-70KM

- In situ dataset (SSS_{Insitu}): Argo (download the corresponding report here)

In the following, $\Delta SSS= SSS_{SAT}- SSS_{Insitu}$ denotes the difference between the satellite and in situ SSS at the colocalized points that form the MDB.

This report presents successively:

The MDB file DataSets (Section 2)

- A short description of the satellite SSS product considered in the match-up (2.1)

- A short description of the In situ SSS dataset considered in the match-up (2.2)

- A short description of the auxiliary geophysical datasets co-localized with SSS pairs (2.3)

- An overview of how the Match-ups were evaluated (2.4)

- An overview of the MDB characteristics for the particular in situ/satellite pairs (2.5)

The major results of the MDB file Analyses (Section 3)

- Spatial Maps of the Time-mean and temporal Std of in situ and satellite SSS and of the ΔSSS (3.1)

- Time series of the monthly averaged mean and Std of in situ and satellite SSS and of the ΔSSS (3.2)

- Zonally-averaged Time-mean and temporal Std of in situ and satellite SSS and of the ΔSSS (3.3)

- Scatterplots of satellite vs in situ SSS by latitudinal bands (3.4)

- Time series of the monthly averaged mean and Std of the ΔSSS sorted by latitudinal bands (3.5)

- ΔSSS sorted as function of geophysical parameters (3.6)

- ΔSSS maps and statistics for different geophysical conditions (3.7)

All analyses are conducted over the Pi-MEP Region specified above and over the full satellite SSS product period.

2 The MDB file datasets

2.1 Satellite SSS product

2.1.1 SMAP-L3-RSS-V3-8DAY-RUNNING-70KM

The version 3.0 70km SMAP-SSS level 3, 8-Day running mean gridded product is the third release of the validated standard mapped sea surface salinity (SSS) data from the NASA Soil Moisture Active Passive (SMAP) observatory produced operationally by Remote Sensing Systems (RSS). Enhancements with this release include: Use of the version 4 L1B SMAP RFI filtered antenna temperatures; Implementation of the geophysical model function from Aquarius version 5 adapted to SMAP; Use of the near real time CCMP wind speed and direction data as ancillary input, and inclusion of IMERG rain rate for the atmospheric liquid cloud water correction and rain flagging; Improved computation of antenna weighted land fraction gland and enhanced correction for land radiation intrusion from antenna sidelobes; Improved SMAP mesh antenna emissivity settings with empirical adjustments to the JPL thermal model. Users should note that significant degradation in the performance is observed if the gain weighted land fraction gland exceeds 1 percent. Because of that, observations with gland greater than 0.8 percent are not used in the Level 3 processing. Daily data files for this product are based on SSS averages spanning an 8-day moving time window. SMAP data begins on April 1,2015 and is ongoing, with a one-month latency in processing and availability. L3 products are global in extent and gridded at 0.25° x 0.25° with an approximate spatial resolution of 70km. The SMAP satellite is in a near-polar orbit at an inclination of 98 degrees and an altitude of 685 km. It has an ascending node time of 6 pm and is sun-synchronous. With its 1000km swath, SMAP achieves global coverage in approximately 3 days, but has an exact orbit repeat cycle of 8 days. On board instruments include a highly sensitive L-band radiometer operating at 1.41GHz and an L-band 1.26GHz radar sensor providing complementary active and passive sensing capabilities. Malfunction of the SMAP scatterometer on 7 July, 2015, has necessitated the use of collocated wind speed, primarily from WindSat, for the surface roughness correction required for the surface salinity retrieval.

We consider only Match-up if the following conditions are met:

- the gain weighted land fraction *gland* do not exceed 0.001 (0.1%)

- the gain weighted sea ice fraction *gice* do not exceed 0.001 (0.1%)

- the sea surface temperature exceeds 278.15 K.

Table 1: Satellite SSS product characteristics

SMAP-L3-RSS-V3-8DAY-RUNNING-70KM	
Spatial resolution	∼70 km gridded at 0.25° x 0.25°
Temporal resolution	8 Day
Temporal coverage	From 2015-03-27 to now
Spatial coverage	Global [-180 180 -90 90]
Data Provider	Remote Sensing Systems (RSS), Santa Rosa, USA
Release Date	2018-10-31
Version	3
User Guide	RSS_SMAP-SSS_V3.0_TechnicalDocumentation.pdf
Documentation	ftp://podaac-ftp.jpl.nasa.gov/allData/smap/docs/V3/
DOI	http://doi.org/10.5067/SMP3A-3SPCS
Data access	http://www.remss.com/missions/smap/

2.2 In situ SSS dataset

Argo is a global array of 3,000 free-drifting profiling floats that measures the temperature and salinity of the upper 2000 m of the ocean. This allows continuous monitoring of the temperature and salinity of the upper ocean, with all data being relayed and made publicly available within hours after collection. The array provides around 100,000 temperature/salinity profiles per year distributed over the global oceans at an average of 3-degree spacing. Only Argo salinity and temperature float data with quality index set to 1 or 2 and data mode set to real time (RT), real time adjusted (RTA) and delayed mode (DM) are considered in the Pi-MEP. Argo floats which may have problems with one or more sensors appearing in the grey list maintained at the Coriolis/GDACs are discarded. Furthermore, Pi-MEP provides an additional list of ∼1000 "suspicious" argo salinity profiles that are also removed before analysis. The upper ocean salinity and temperature values recorded between 0m and 10m depth are considered as Argo sea surface salinities (SSS) and sea surface temperatures (SST). These data were collected and made freely available by the international Argo project and the national programs that contribute to it (Argo (2000)).

2.3 Auxiliary geophysical datasets

Additional EO datasets are used to characterize the geophysical conditions at the in situ/satellite SSS pair measurement locations and time, and 10 days prior the measurements to get an estimate of the geophysical condition and history. As discussed in Boutin et al. (2016), the presence of vertical gradients in, and horizontal variability of, sea surface salinity indeed complicates comparison of satellite and in situ measurements. The additional EO data are used here to get a first estimates of conditions for which L-band satellite SSS measured in the first centimeters of the upper ocean within a 50-150 km diameter footprint might differ from pointwise in situ measurements performed in general between 10 and 5 m depth below the surface. The spatio-temporal variability of SSS within a satellite footprint (50–150 km) is a major issue for satellite SSS validation in the vicinity of river plumes, frontal zones, and significant precipitation. Rainfall can in some cases produce vertical salinity gradients exceeding 1 pss m^{-1}; consequently, it is recommended that satellite and in situ SSS measurements less than 3–6 h after rain events should be considered with care when used in satellite calibration/validation analyses. To identify such situation, the Pi-MEP test platform is first using CMORPH products to characterize the local

value and history of rain rate and ASCAT gridded data are used to characterize the local surface wind speed and history. For validation purpose, the ISAS monthly SSS in situ analysed fields at 5 m depth are collocated and compared with the satellite SSS products. The use of ISAS is motivated by the fact that it is used in the SMOS L2 official validation protocol in which systematic comparisons of SMOS L2 retrieved SSS with ISAS are done. In complement to ISAS, monthly std climatological fields from the World Ocean Atlas (WOA13) at the match-up pairs location and date are also used to have an a priori information of the local SSS variability.

2.3.1 CMORPH

Precipitation are estimated using the CMORPH 3-hourly products at $1/4°$ resolution (Joyce et al. (2004)). CMORPH (CPC MORPHing technique) produces global precipitation analyses at very high spatial and temporal resolution. This technique uses precipitation estimates that have been derived from low orbiter satellite microwave observations exclusively, and whose features are transported via spatial propagation information that is obtained entirely from geostationary satellite IR data. At present NOAA incorporate precipitation estimates derived from the passive microwaves aboard the DMSP 13, 14 and 15 (SSM/I), the NOAA-15, 16, 17 and 18 (AMSU-B), and AMSR-E and TMI aboard NASA's Aqua, TRMM and GPM spacecraft, respectively. These estimates are generated by algorithms of Ferraro (1997) for SSM/I, Ferraro et al. (2000) for AMSU-B and Kummerow et al. (2001) for TMI. Note that this technique is not a precipitation estimation algorithm but a means by which estimates from existing microwave rainfall algorithms can be combined. Therefore, this method is extremely flexible such that any precipitation estimates from any microwave satellite source can be incorporated.

With regard to spatial resolution, although the precipitation estimates are available on a grid with a spacing of 8 km (at the equator), the resolution of the individual satellite-derived estimates is coarser than that - more on the order of 12 x 15 km or so. The finer "resolution" is obtained via interpolation.

In effect, IR data are used as a means to transport the microwave-derived precipitation features during periods when microwave data are not available at a location. Propagation vector matrices are produced by computing spatial lag correlations on successive images of geostationary satellite IR which are then used to propagate the microwave derived precipitation estimates. This process governs the movement of the precipitation features only. At a given location, the shape and intensity of the precipitation features in the intervening half hour periods between microwave scans are determined by performing a time-weighting interpolation between microwave-derived features that have been propagated forward in time from the previous microwave observation and those that have been propagated backward in time from the following microwave scan. NOAA refer to this latter step as "morphing" of the features.

For the present Pi-MEP products, we only considered the 3-hourly products at 1/4 degree resolution. The entire CMORPH record (December 2002-present) for 3-hourly, 1/4 degree lat/lon resolution can be found at: `ftp://ftp.cpc.ncep.noaa.gov/precip/CMORPH_V1.0/RAW/`. CMORPH estimates cover a global belt (-180°W to 180°E) extending from 60°S to 60°N latitude and are available for the complete period of the Pi-MEP core datasets (Jan 2010-now).

2.3.2 ASCAT

Advanced SCATterometer (ASCAT) daily data produced and made available at Ifremer/CERSAT on a 0.25°x0.25° resolution grid (Bentamy and Fillon (2012)) since March 2007 are used to characterize the mean daily wind at the match-up pair location as well as the wind history during the 10-days period preceding the in situ measurement date. These wind fields are calculated based on a geostatistical method with external drift. Remotely sensed data from ASCAT are considered

as observations while those from numerical model analysis (ECMWF) are associated with the external drift. The spatial and temporal structure functions for wind speed, zonal and meridional wind components are estimated from ASCAT retrievals. Furthermore, the new procedure includes a temporal interpolation of the retrievals based on the complex empirical orthogonal function (CEOF) approach, in order to enhance the sampling length of the scatterometer observations. The resulting daily wind fields involves the main known surface wind patterns as well as some variation modes associated with temporal and spatial moving features. The accuracy of the gridded winds was investigated through comparisons with moored buoy data in Bentamy et al. (2012) and resulted in rms differences for wind speed and direction are about 1.50 m.s^{-1} and 20°.

2.3.3 ISAS

The In Situ Analysis System (ISAS), as described in Gaillard et al. (2016) is a data based re-analysis of temperature and salinity fields over the global ocean. It was initially designed to synthesize the temperature and salinity profiles collected by the Argo program. It has been later extended to accommodate all type of vertical profile as well as time series. ISAS gridded fields are entirely based on in-situ measurements. The methodology and configuration have been conceived to preserve as much as possible the data information content and resolution. ISAS is developed and run in a research laboratory (LOPS) in close collaboration with Coriolis, one of Argo Global Data Assembly Center and unique data provider for the Mercator operational oceanography system. At the moment the period covered starts in 2002 and only the upper 2000 m are considered. The gridded fields were produced over the global ocean 70°N–70°S on a 1/2° grid by the ISAS project with datasets downloaded from the Coriolis data center (for more details on ISAS see Gaillard et al. (2009)). In the Pi-MEP, the product in used is the INSITU_GLO_TS_OA_NRT_OBSERVATIONS_013_002_a v6.2 NRT derived at the Coriolis data center and provided by Copernicus (www.marine.copernicus.eu/documents/PUM/CMEMS-INS-PUM-013-002-ab.pdf). The major contribution to the data set is from Argo array of profiling floats, reaching an approximate resolution of one profile every 10-days and every 3-degrees over the satellite SSS period (http://www.umr-lops.fr/SNO-Argo/Products/ISAS-T-S-fields/); in this version SSS from ship of opportunity thermosalinographs are not used, so that we can consider SMOS SSS validation using these measurements independent of ISAS. The ISAS optimal interpolation involves a structure function modeled as the sum of two Gaussian functions, each associated with specific time and space scales, resulting in a smoothing over typically 3 degrees. The smallest scale which can be retrieved with ISAS analysis is not smaller than 300–500 km (Kolodziejczyk et al. (2015)). For validation purpose, the ISAS monthly SSS fields at 5 m depth are collocated and compared with the satellite SSS products and included in the Pi-MEP Match-up files. In addition, the "percentage of variance" fields (PCTVAR) contained in the ISAS analyses provide information on the local variability of in situ SSS measurements within 1/2°x1/2° boxes.

2.3.4 World Ocean Atlas Climatology

The World Ocean Atlas 2013 version 2 (WOA13 V2) is a set of objectively analyzed (1° grid) climatological fields of in situ temperature, salinity and other variables provided at standard depth levels for annual, seasonal, and monthly compositing periods for the World Ocean. It also includes associated statistical fields of observed oceanographic profile data interpolated to standard depth levels on 5°, 1°, and 0.25° grids. We use these fields in complement to ISAS to characterize the climatological fields (annual mean and std) at the match-up pairs location and date.

2.4   Overview of the Match-ups generation method

The match-up production is basically a three steps process:

1. preparation of the input in situ and satellite data, and,

2. co-localization of satellite products with in situ SSS measurements.

3. co-localization of the in situ/satellite pair with auxiliary information.

 In the following, we successively detail the approaches taken for these different steps.

2.4.1   In Situ/Satellite data filtering

The first step consist in filtering Argoin situ dataset using the quality flags as described in 2.2 so that only valid salinity data remains in the produced match-ups.

 For high-spatial resolution in situ SSS measurements such as the Thermo-SalinoGraph (TSG) SSS data from research vessels, Voluntary Observing Ships (VOS) or sailing ships, as well as SSS data from surface drifters, an additional spatial-filtering step is performed on the in situ data that will be in fine compared to the satellite SSS products. If R_{sat} is the spatial resolution of the satellite SSS product (L2 to L3-L4), we keep the in situ data at the original spatial resolution but we also estimate for all spatio-temporal samples a running median filtered SSS applied to all neighbouring in situ SSS data acquired within a distance of $R_{sat}/2$ from a given in situ acquisition. Both the original and the filtered data are finally stored in the MDB files.

 Only for satellite L2 SSS data, a third step consist in filtering spurious data using the flags and associated recommendation as provided by the official data centers and described in 2.1.

2.4.2   In Situ/Satellite Co-localization

In this step, each SSS satellite acquisition is co-localized with the filtered in situ measurements. The method used for co-localization differ if the satellite SSS is a swath product (so-called Level 2-types) or a time-space composite product (so-called Level 3/level 4-types).

- For L2 SSS swath data :

  If R_{sat} is the spatial resolution of the satellite swath SSS product, for each in situ data sample collected in the Pi-MEP database, the platform searches for all satellite SSS data found at grid nodes located within a radius of $R_{sat}/2$ from the in situ data location and acquired with a time-lag from the in situ measurement date that is less or equal than $\pm$ 12 hours. If several satellite SSS samples are found to meet these criteria, the final satellite SSS match-up point is selected to be the closest in time from the in situ data measurement date. The final spatial and temporal lags between the in situ and satellite data are stored in the MDB files.

- For L3 and L4 composite SSS products :

  If R_{sat} is the spatial resolution of the composite satellite SSS product and D the period over which the composite product was built (e.g., periods of 1, 7, 8, 9, 10, 18 days, 1 month, etc..) with central time to, for each in situ data sample collected in the Pi-MEP database during period D, the platform searches for all satellite SSS data of the composite product found at grid nodes located within a radius of $R_{sat}/2$ from the in situ data location. If several satellite SSS product samples are found to meet these criteria, the final satellite SSS match-up point is chosen to be the composite SSS with central time to which is the closest in time from the in situ data measurement date. The final spatial and temporal lags between the in situ and satellite data are stored in the MDB files.

2.4.3 MDB pair Co-localization with auxiliary data and complementary information

MDB data consist of satellite and in-situ SSS pair datasets but also of auxiliary geophysical parameters such as local and history of wind speed and rain rates, as well as various information (climatology, distance to coast, mixed layer depth, barrier layer thickness, etc) that can be derived from in situ data and which are included in the final match-up files. The collocation of auxiliary parameters and additional information is done for each filtered in-situ SSS measurement contained in the match-up files as follows :

If t_{insitu} is the time/date at which the in situ measurement is performed, we collect:

- The ASCAT wind speed product of the same day than t_{insitu} found at the ASCAT $1/4°$ grid node with closest distance from the in situ data location and the time series of the ASCAT wind speed at the same node for the 10 days prior the in situ measurement day.

- If the in situ data is located within the 60°N-60°S band, we select the CMORPH 3-hourly product the closest in time from tin situ and found at the CMORPH $1/4°$ grid node with closest distance from the in situ data location. We then store the time series of the CMORPH rain rate at the same node for the 10 days prior the in situ measurement time.

For the given month/year of the in situ data, we select the ISAS and WOA fields for the same month (and same year for ISAS fields) and take the SSS analysis (monthly mean, std) found at the closest grid node from the in situ measurement.

The distance from the in situ SSS data location to the nearest coast is evaluated and provided in km. We use a distance-to-coast map at $1/4°$ resolution where small islands have been removed.

When vertical profiles of salinity (S) and temperature (T) are made available from the in situ measurements used to build the match-up (Argo or sea mammals), the following variables are included into each satellite/in situ match-up file:

1. The vertical distribution of pressure at which the profile were measured,

2. The vertical S(z) and T(z) profiles,

3. The vertical potential density anomaly profile $\sigma_0(z)$,

4. The Mixed Layer Depth (MLD). The MLD is defined here as the depth where the potential density has increased from the reference depth (10 meter) by a threshold equivalent to $0.2°C$ decrease in temperature at constant salinity: $\sigma_0 = \sigma_{010m} + \Delta\sigma_0$ with $\Delta\sigma_0 = \sigma_0(\theta_{10m} - 0.2, S_{10m}) - \sigma_0(\theta_{10m}, S_{10m})$ where θ_{10m} and S_{10m} are the temperature and salinity at the reference depth (i.e. 10 m) (de Boyer Montégut et al. (2004), de Boyer Montégut et al. (2007)).

5. The Top of the Thermocline Depth (TTD) is defined as the depth at which temperature decreases from its 10 m value by $0.2°C$.

6. The Barrier Layer if present, is defined as the intermediate layer between the top of the thermocline and the bottom of the density mixed-layer and its thickness (BLT) is defined as the difference between the MLD and the TTD.

7. The vertical profile of the buoyancy frequency $N^2(z)$

The resulting match-ups files are serialized as NetCDF-4 files whose structure depends on the origin of the in-situ data they contain.

2.4.4 Content of the Match-Up NetCDF files

netcdf pimep-mdb_smap-l3-rss-v3-8dr-70km_argo_TIMEID_v01 {
dimensions:
      N_prof = 944 ;
      N_LEVELS = 499 ;
      N_DAYS_WIND = 10 ;
      N_3H_RAIN = 80 ;
      TIME_Sat = UNLIMITED ; // (1 currently)
variables:
float DATE_ARGO(N_prof) ;
      DATE_ARGO:long_name = "Date of Argo profile" ;
      DATE_ARGO:units = "days since 1990-01-01 00:00:00" ;
      DATE_ARGO:standard_name = "time" ;
      DATE_ARGO:_FillValue = -999.f ;
float LATITUDE_ARGO(N_prof) ;
      LATITUDE_ARGO:long_name = "Latitude of Argo profile" ;
      LATITUDE_ARGO:units = "degrees_north" ;
      LATITUDE_ARGO:valid_min = -90. ;
      LATITUDE_ARGO:valid_max = 90. ;
      LATITUDE_ARGO:standard_name = "latitude" ;
      LATITUDE_ARGO:_FillValue = -999.f ;
float LONGITUDE_ARGO(N_prof) ;
      LONGITUDE_ARGO:long_name = "Longitude of Argo profile" ;
      LONGITUDE_ARGO:units = "degrees_east" ;
      LONGITUDE_ARGO:valid_min = -180. ;
      LONGITUDE_ARGO:valid_max = 180. ;
      LONGITUDE_ARGO:standard_name = "longitude" ;
      LONGITUDE_ARGO:_FillValue = -999.f ;
float SSS_DEPTH_ARGO(N_prof) ;
      SSS_DEPTH_ARGO:long_name = "Sea water pressure at Argo float location (equals 0 at sea level)" ;
      SSS_DEPTH_ARGO:units = "decibar" ;
      SSS_DEPTH_ARGO:standard_name = "sea_water_pressure" ;
      SSS_DEPTH_ARGO:_FillValue = -999.f ;
float SSS_ARGO(N_prof) ;
      SSS_ARGO:long_name = "Argo SSS" ;
      SSS_ARGO:units = "1" ;
      SSS_ARGO:salinity_scale = "Practical Salinity Scale(PSS-78)" ;
      SSS_ARGO:standard_name = "sea_water_salinity" ;
      SSS_ARGO:_FillValue = -999.f ;
float SST_ARGO(N_prof) ;
      SST_ARGO:long_name = "Argo SST" ;
      SST_ARGO:units = "degree Celsius" ;
      SST_ARGO:standard_name = "sea_water_temperature" ;
      SST_ARGO:_FillValue = -999.f ;
float DELAYED_MODE_ARGO(N_prof) ;
      DELAYED_MODE_ARGO:long_name = "Argo data mode (delayed mode = 1, real time =0) " ;

DELAYED_MODE_ARGO:units = "1" ;
DELAYED_MODE_ARGO:_FillValue = -999.f ;
float DISTANCE_TO_COAST_ARGO(N_prof) ;
DISTANCE_TO_COAST_ARGO:long_name = "Distance to coasts at Argo float location"
;
DISTANCE_TO_COAST_ARGO:units = "km" ;
DISTANCE_TO_COAST_ARGO:_FillValue = -999.f ;
float PLATFORM_NUMBER_ARGO(N_prof) ;
PLATFORM_NUMBER_ARGO:long_name = "Argo float unique identifier" ;
PLATFORM_NUMBER_ARGO:conventions = "WMO float identifier : A9IIIII" ;
PLATFORM_NUMBER_ARGO:units = "1" ;
PLATFORM_NUMBER_ARGO:_FillValue = -999.f ;
float PSAL_ARGO(N_prof, N_LEVELS) ;
PSAL_ARGO:long_name = "Argo salinity profile" ;
PSAL_ARGO:units = "1" ;
PSAL_ARGO:salinity_scale = "Practical Salinity Scale (PSS-78)" ;
PSAL_ARGO:standard_name = "sea_water_salinity" ;
PSAL_ARGO:_FillValue = -999.f ;
float TEMP_ARGO(N_prof, N_LEVELS) ;
TEMP_ARGO:long_name = "Argo temperature profile" ;
TEMP_ARGO:units = "degree Celsius" ;
TEMP_ARGO:standard_name = "sea_water_temperature" ;
TEMP_ARGO:_FillValue = -999.f ;
float PRES_ARGO(N_prof, N_LEVELS) ;
PRES_ARGO:long_name = "Argo pressure profile" ;
PRES_ARGO:units = "decibar" ;
PRES_ARGO:standard_name = "sea_water_pressure" ;
PRES_ARGO:_FillValue = -999.f ;
float RHO_ARGO(N_prof, N_LEVELS) ;
RHO_ARGO:long_name = "Argo in-situ density profile" ;
RHO_ARGO:units = "kg/m" ;
RHO_ARGO:_FillValue = -999.f ;
float SIGMA0_ARGO(N_prof, N_LEVELS) ;
SIGMA0_ARGO:long_name = "Argo potential density anomaly profile" ;
SIGMA0_ARGO:units = "kg/m^3" ;
SIGMA0_ARGO:_FillValue = -999.f ;
float N2_ARGO(N_prof, N_LEVELS) ;
N2_ARGO:long_name = "Argo buoyancy frequency profile" ;
N2_ARGO:units = "1/s^2" ;
N2_ARGO:_FillValue = -999.f ;
float MLD_ARGO(N_prof) ;
MLD_ARGO:long_name = "Mixed Layer Depth (MLD) calculated from Argo profile (depth
where $\sigma_0 = \sigma_{010m} + \Delta\sigma_0$ with $\Delta\sigma_0 = \sigma_0(\theta_{10m} - 0.2, S_{10m}) - \sigma_0(\theta_{10m}, S_{10m})$)" ;
MLD_ARGO:units = "m" ;
MLD_ARGO:_FillValue = -999.f ;
float TTD_ARGO(N_prof) ;
TTD_ARGO:long_name = "Top of Thermocline Depth (TTD) calculated from Argo profile
(depth where $\theta = \theta_{10m} - 0.2$)" ;
TTD_ARGO:units = "m" ;

TTD_ARGO:_FillValue = -999.f ;
float BLT_ARGO(N_prof) ;
     BLT_ARGO:long_name = "Barrier Layer Thickness (TTD-MLD)" ;
     BLT_ARGO:units = "m" ;
     BLT_ARGO:_FillValue = -999.f ;
float DATE_Satellite_product(TIME_Sat) ;
     DATE_Satellite_product:long_name = "Central time of satellite SSS file" ;
     DATE_Satellite_product:units = "days since 1990-01-01 00:00:00" ;
     DATE_Satellite_product:standard_name = "time" ;
float LATITUDE_Satellite_product(N_prof) ;
     LATITUDE_Satellite_product:long_name = "Satellite product latitude at Argo float location" ;
     LATITUDE_Satellite_product:units = "degrees_north" ;
     LATITUDE_Satellite_product:valid_min = -90. ;
     LATITUDE_Satellite_product:valid_max = 90. ;
     LATITUDE_Satellite_product:standard_name = "latitude" ;
     LATITUDE_Satellite_product:_FillValue = -999.f ;
float LONGITUDE_Satellite_product(N_prof) ;
     LONGITUDE_Satellite_product:long_name = "Satellite product longitude at Argo float location" ;
     LONGITUDE_Satellite_product:units = "degrees_east" ;
     LONGITUDE_Satellite_product:valid_min = -180. ;
     LONGITUDE_Satellite_product:valid_max = 180. ;
     LONGITUDE_Satellite_product:standard_name = "longitude" ;
     LONGITUDE_Satellite_product:_FillValue = -999.f ;
float SSS_Satellite_product(N_prof) ;
     SSS_Satellite_product:long_name = "Satellite product SSS at Argo float location" ;
     SSS_Satellite_product:units = "1" ;
     SSS_Satellite_product:salinity_scale = "Practical Salinity Scale(PSS-78)" ;
     SSS_Satellite_product:standard_name = "sea_surface_salinity" ;
     SSS_Satellite_product:_FillValue = -999.f ;
float SST_Satellite_product(N_prof) ;
     SST_Satellite_product:long_name = "Satellite product SST at Argo float location" ;
     SST_Satellite_product:units = "degree Celsius" ;
     SST_Satellite_product:standard_name = "sea_surface_temperature" ;
     SST_Satellite_product:_FillValue = -999.f ;
float Spatial_lags(N_prof) ;
     Spatial_lags:long_name = "Spatial lag between Argo float location and satellite SSS product pixel center" ;
     Spatial_lags:units = "km" ;
     Spatial_lags:_FillValue = -999.f ;
float Time_lags(N_prof) ;
     Time_lags:long_name = "Temporal lag between Argo float time and satellite SSS product central time" ;
     Time_lags:units = "days" ;
     Time_lags:_FillValue = -999.f ;
float ROSSBY_RADIUS_at_ARGO(N_prof) ;
     ROSSBY_RADIUS_at_ARGO:long_name = "Baroclinic Rossby radius of deformation (Chelton et al., 1998) at Argo float location" ;

ROSSBY_RADIUS_at_ARGO:units = "km" ;
ROSSBY_RADIUS_at_ARGO:_FillValue = -999.f ;
float Ascat_daily_wind_at_ARGO(N_prof) ;
Ascat_daily_wind_at_ARGO:long_name = "Daily Ascat wind speed module at Argo float location" ;
Ascat_daily_wind_at_ARGO:units = "m/s" ;
Ascat_daily_wind_at_ARGO:_FillValue = -999.f ;
float CMORPH_3h_Rain_Rate_at_ARGO(N_prof) ;
CMORPH_3h_Rain_Rate_at_ARGO:long_name = "3-hourly CMORPH rain rate at Argo float location" ;
CMORPH_3h_Rain_Rate_at_ARGO:units = "mm/3h" ;
CMORPH_3h_Rain_Rate_at_ARGO:_FillValue = -999.f ;
float Ascat_10_prior_days_wind_at_ARGO(N_prof, N_DAYS_WIND) ;
Ascat_10_prior_days_wind_at_ARGO:long_name = "Prior 10 days time series of Ascat wind speed module at Argo float location" ;
Ascat_10_prior_days_wind_at_ARGO:units = "m/s" ;
Ascat_10_prior_days_wind_at_ARGO:_FillValue = -999.f ;
float CMORPH_10_prior_days_Rain_Rate_at_ARGO(N_prof, N_3H_RAIN) ;
CMORPH_10_prior_days_Rain_Rate_at_ARGO:long_name = "Prior 10 days times series of 3-hourly CMORPH Rain Rate at Argo float location" ;
CMORPH_10_prior_days_Rain_Rate_at_ARGO:units = "mm/3h" ;
CMORPH_10_prior_days_Rain_Rate_at_ARGO:_FillValue = -999.f ;
float SSS_ISAS_at_ARGO(N_prof) ;
SSS_ISAS_at_ARGO:long_name = "ISAS SSS (5m depth) at Argo float location" ;
SSS_ISAS_at_ARGO:units = "1" ;
SSS_ISAS_at_ARGO:salinity_scale = "Practical Salinity Scale(PSS-78)" ;
SSS_ISAS_at_ARGO:standard_name = "sea_water_salinity" ;
SSS_ISAS_at_ARGO:_FillValue = -999.f ;
float SSS_PCTVAR_ISAS_at_ARGO(N_prof) ;
SSS_PCTVAR_ISAS_at_ARGO:long_name = "Error on ISAS SSS (5m depth) at Argo float location (% variance)" ;
SSS_PCTVAR_ISAS_at_ARGO:units = "%" ;
SSS_PCTVAR_ISAS_at_ARGO:_FillValue = -999.f ;
float SSS_WOA13_at_ARGO(N_prof) ;
SSS_WOA13_at_ARGO:long_name = "WOA 2013 (DECAV-1deg) SSS (0m depth) at Argo float location" ;
SSS_WOA13_at_ARGO:units = "1" ;
SSS_WOA13_at_ARGO:salinity_scale = "Practical Salinity Scale(PSS-78)" ;
SSS_WOA13_at_ARGO:standard_name = "sea_surface_salinity" ;
SSS_WOA13_at_ARGO:_FillValue = -999.f ;
float SSS_STD_WOA13_at_ARGO(N_prof) ;
SSS_STD_WOA13_at_ARGO:long_name = "WOA 2013 (DECAV-1deg) SSS STD (0m depth) at Argo float location " ;
SSS_STD_WOA13_at_ARGO:units = "1" ;
SSS_STD_WOA13_at_ARGO:_FillValue = -999.f ;
float SSS_ISAS15_at_ARGO(N_prof) ;
SSS_ISAS15_at_ARGO:long_name = "Monthly ISAS-15 SSS (5m depth) at Argo float location" ;
SSS_ISAS15_at_ARGO:units = "1" ;

SSS_ISAS15_at_ARGO:salinity_scale = "Practical Salinity Scale (PSS-78)" ;
SSS_ISAS15_at_ARGO:standard_name = "sea_water_salinity" ;
SSS_ISAS15_at_ARGO:_FillValue = -999.f ;
float SSS_PCTVAR_ISAS15_at_ARGO(N_prof) ;
SSS_PCTVAR_ISAS15_at_ARGO:long_name = "Error on monthly ISAS-15 SSS (5m depth) at Argo float location (% variance)" ;
SSS_PCTVAR_ISAS15_at_ARGO:units = "%" ;
SSS_PCTVAR_ISAS15_at_ARGO:_FillValue = -999.f ;
float SSS_WOA18_at_ARGO(N_prof) ;
SSS_WOA18_at_ARGO:long_name = "Monthly WOA 2018 (DECAV-1deg) SSS (0m depth) at Argo float location" ;
SSS_WOA18_at_ARGO:units = "1" ;
SSS_WOA18_at_ARGO:salinity_scale = "Practical Salinity Scale (PSS-78)" ;
SSS_WOA18_at_ARGO:standard_name = "sea_surface_salinity" ;
SSS_WOA18_at_ARGO:_FillValue = -999.f ;
float SSS_STD_WOA18_at_ARGO(N_prof) ;
SSS_STD_WOA18_at_ARGO:long_name = "Monthly WOA 2018 (DECAV-1deg) SSS STD (0m depth) at Argo float location " ;
SSS_STD_WOA18_at_ARGO:units = "1" ;
SSS_STD_WOA18_at_ARGO:_FillValue = -999.f ;
float SEA_ICE_CONCENTRATION_at_ARGO(N_prof) ;
SEA_ICE_CONCENTRATION_at_ARGO:long_name = "Daily sea ice area fraction (EU-METSAT OSI-SAF OSI-450) at Argo float location (%)" ;
SEA_ICE_CONCENTRATION_at_ARGO:units = "1" ;
SEA_ICE_CONCENTRATION_at_ARGO:standard_name = "sea_ice_area_fraction" ;
SEA_ICE_CONCENTRATION_at_ARGO:_FillValue = -999.f ;
float CCMP_6h_Wind_Speed_at_ARGO(N_prof) ;
CCMP_6h_Wind_Speed_at_ARGO:long_name = "6-hourly CCMP wind speed at Argo float location" ;
CCMP_6h_Wind_Speed_at_ARGO:units = "m s-1" ;
CCMP_6h_Wind_Speed_at_ARGO:standard_name = "wind_speed" ;
CCMP_6h_Wind_Speed_at_ARGO:_FillValue = -999.f ;
float CCMP_10_prior_days_Wind_Speed_at_ARGO(N_prof, N_DAYS_WIND_CCMP) ;
CCMP_10_prior_days_Wind_Speed_at_ARGO:long_name = "Prior 10 days time series of CCMP wind speed at Argo float location" ;
CCMP_10_prior_days_Wind_Speed_at_ARGO:units = "m s-1" ;
CCMP_10_prior_days_Wind_Speed_at_ARGO:standard_name = "wind_speed" ;
CCMP_10_prior_days_Wind_Speed_at_ARGO:_FillValue = -999.f ;
float CDM_GLOBCOLOUR_at_ARGO(N_prof) ;
CDM_GLOBCOLOUR_at_ARGO:long_name = "8-day Coloured dissolved and detrital organic materials - mean of the binned pixels at Argo float location" ;
CDM_GLOBCOLOUR_at_ARGO:units = "m-1" ;
CDM_GLOBCOLOUR_at_ARGO:standard_name = "volume_absorption_coefficient_of_radiative_flux_in_sea_water" ;
CDM_GLOBCOLOUR_at_ARGO:_FillValue = -999.f ;
float CHL1_GLOBCOLOUR_at_ARGO(N_prof) ;
CHL1_GLOBCOLOUR_at_ARGO:long_name = "8-day Chlorophyll concentration - mean of the binned pixels at Argo float location" ;
CHL1_GLOBCOLOUR_at_ARGO:units = "mg m-3" ;

CHL1_GLOBCOLOUR_at_ARGO:standard_name = "mass_concentration_of_chlorophyll_a_in_sea_water"
;
CHL1_GLOBCOLOUR_at_ARGO:_FillValue = -999.f ;
float EVAPORATION_OAFLUX_at_ARGO(N_prof) ;
EVAPORATION_OAFLUX_at_ARGO:long_name = "Daily mean evaporation rate (OAFlux)
at Argo float location" ;
EVAPORATION_OAFLUX_at_ARGO:units = "cm year-1" ;
EVAPORATION_OAFLUX_at_ARGO:_FillValue = -999.f ;
float SSS_SCRIPPS_at_ARGO(N_prof) ;
SSS_SCRIPPS_at_ARGO:long_name = "Argo gridded monthly mean SSS (0m depth) from
SCRIPPS (Roemmich-Gilson) at Argo float location" ;
SSS_SCRIPPS_at_ARGO:units = "1" ;
SSS_SCRIPPS_at_ARGO:salinity_scale = "Practical Salinity Scale (PSS-78)" ;
SSS_SCRIPPS_at_ARGO:standard_name = "sea_water_salinity" ;
SSS_SCRIPPS_at_ARGO:_FillValue = -999.f ;
float SSS_IPRC_at_ARGO(N_prof) ;
SSS_IPRC_at_ARGO:long_name = "Argo gridded monthly mean SSS (0m depth) from
IPRC at Argo float location" ;
SSS_IPRC_at_ARGO:units = "1" ;
SSS_IPRC_at_ARGO:salinity_scale = "Practical Salinity Scale (PSS-78)" ;
SSS_IPRC_at_ARGO:standard_name = "sea_water_salinity" ;
SSS_IPRC_at_ARGO:_FillValue = -999.f ;
float SST_AVHRR_at_ARGO(N_prof) ;
SST_AVHRR_at_ARGO:long_name = "Daily OI AVHRR-only v2 SST (Reynolds et al.,
2007) at Argo float location" ;
SST_AVHRR_at_ARGO:units = "degree Celsius" ;
SST_AVHRR_at_ARGO:standard_name = "sea_water_temperature" ;
SST_AVHRR_at_ARGO:_FillValue = -999.f ;
float U_EKMAN_GLOBCURRENT_at_ARGO(N_prof) ;
U_EKMAN_GLOBCURRENT_at_ARGO:long_name = "15m depth Ekman current veloc-
ity: zonal component at Argo float location" ;
U_EKMAN_GLOBCURRENT_at_ARGO:units = "m s-1" ;
U_EKMAN_GLOBCURRENT_at_ARGO:_FillValue = -999.f ;
float V_EKMAN_GLOBCURRENT_at_ARGO(N_prof) ;
V_EKMAN_GLOBCURRENT_at_ARGO:long_name = "15m depth Ekman current veloc-
ity: meridian component at Argo float location" ;
V_EKMAN_GLOBCURRENT_at_ARGO:units = "m s-1" ;
V_EKMAN_GLOBCURRENT_at_ARGO:_FillValue = -999.f ;
float U_GEOSTROPHIC_GLOBCURRENT_at_ARGO(N_prof) ;
U_GEOSTROPHIC_GLOBCURRENT_at_ARGO:long_name = "Absolute geostrophic ve-
locity: zonal component at Argo float location" ;
U_GEOSTROPHIC_GLOBCURRENT_at_ARGO:units = "m s-1" ;
U_GEOSTROPHIC_GLOBCURRENT_at_ARGO:_FillValue = -999.f ;
float V_GEOSTROPHIC_GLOBCURRENT_at_ARGO(N_prof) ;
V_GEOSTROPHIC_GLOBCURRENT_at_ARGO:long_name = "Absolute geostrophic ve-
locity: meridian component at Argo float location" ;
V_GEOSTROPHIC_GLOBCURRENT_at_ARGO:units = "m s-1" ;
V_GEOSTROPHIC_GLOBCURRENT_at_ARGO:_FillValue = -999.f ;

```
    // global attributes:
      :Conventions = "CF-1.6" ;
      :title = "ARGO Match-Up Database" ;
      :Satellite_product_name = "SMAP-L3-RSS-V3-8DAY-RUNNING-70KM" ;
      :Satellite_product_spatial_resolution = "70 km" ;
      :Satellite_product_temporal_resolution = "8 day running" ;
      :Satellite_product_filename = " v3/8day_running/70km/2015/086/RSS_smap_SSS_L3_8day_running_70km_2015_090_FNL_v03.0.nc"
;
      :Match-Up_spatial_window_radius_in_km = 35;
      :Match-Up_temporal_window_radius_in_days = 0.5;
      :start_time = "20100114T000005Z" ;
      :stop_time = "20100118T235026Z" ;
      :northernmost_latitude = 77.676f ;
      :sourthenmost_latitude = -66.423f ;
      :westernmost_longitude = -179.219f ;
      :easternmost_longitude = 179.199f ;
      :geospatial_lat_units = "degrees north" ;
      :geospatial_lat_resolution = "70 km" ;
      :geospatial_lon_units = "degrees east" ;
      :geospatial_lon_resolution = "70 km" ;
      :institution = "ESA-IFREMER-ODL" ;
      :project_name = "SMOS Pilote Mission Exploitation Platfrom (Pi-MEP) for salinity" ;
      :project_url = "https://pimep-project.odl.bzh" ;
      :license = "Pi-MEP data use is free and open" ;
      :product_version = "1.0" ;
      :keywords = "Oceans > Ocean Salinity > Sea Surface Salinity" ;
      :acknowledgment = "Please acknowledge the use of these data with the following statement:
These data were provided by SMOS Pilote Mission Exploitation Platfrom (Pi-MEP) for salinity"
;
      :source = "v3/8day_running/70km/2015/086/RSS_smap_SSS_L3_8day_running_70km_2015_090_FNL_v03.0.nc" ;
      :In_situ_data_source = "ftp://ftp.ifremer.fr/ifremer/argo/geo/" ;
      :references = "https://pimep-project.odl.bzh" ;
      :history = "Processed on 2018-04-18 using MDB_generator" ;
      :date_created = "2018-04-18 17:09:30" ;
}
```

2.5 MDB characteristics for the particular in situ/satellite pairs

2.5.1 Number of paired SSS data as a function of time and distance to coast
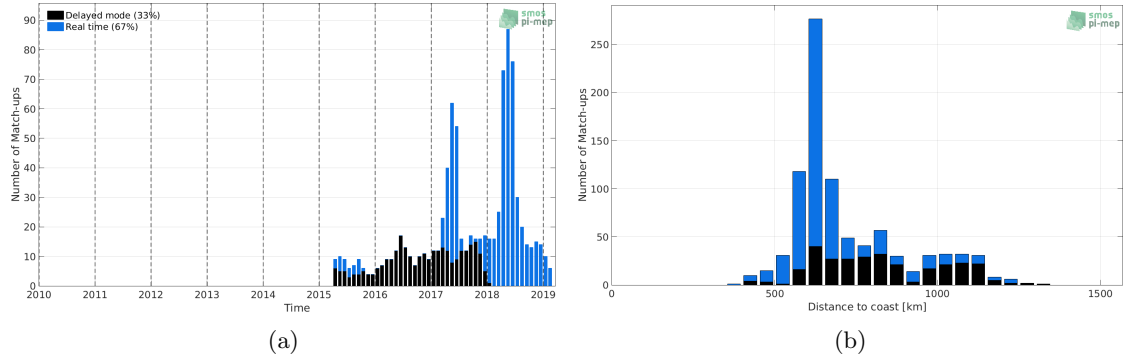
Figure 1: Number of match-ups between Argo and SMAP-L3-RSS-V3-8DAY-RUNNING-70KM SSS as a function of time (a) and as function of the distance to coast (b) over the Congo river plume Pi-MEP region and for the full satellite product period.

2.5.2 Histograms of the SSS match-ups
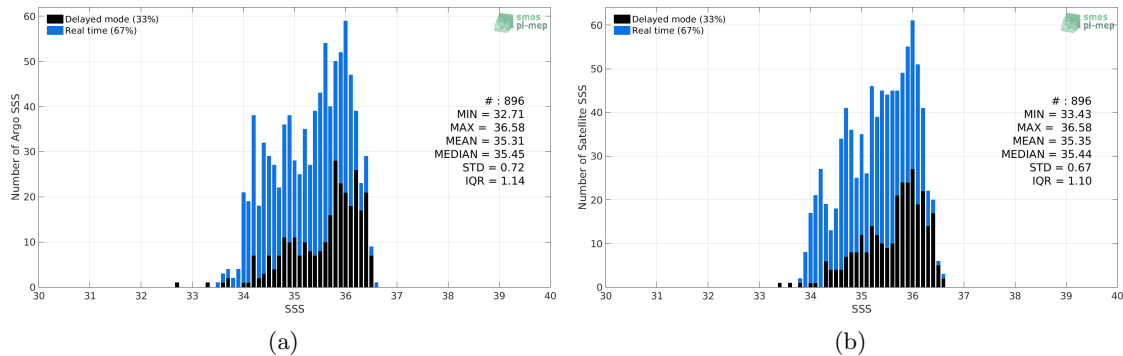
Figure 2: Histograms of SSS from Argo (a) and SMAP-L3-RSS-V3-8DAY-RUNNING-70KM (b) considering all match-up pairs per bins of 0.1 over the Congo river plume Pi-MEP region and for the full satellite product period.

2.5.3 Distribution of in situ SSS depth measurements

(a)   (b)
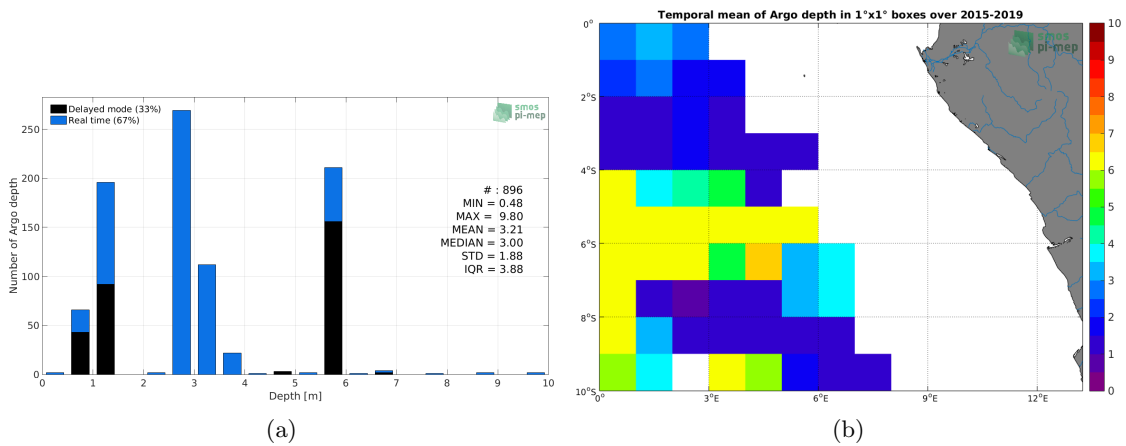
Figure 3: Histograms of the depth of the upper level SSS measurements from Argo in the Match-up DataBase for the Congo river plume Pi-MEP region (a) and temporal mean spatial distribution of pressure of the in situ SSS data over 1°x1° boxes and for the full satellite product period (b).

2.5.4 Spatial Distribution of Match-ups
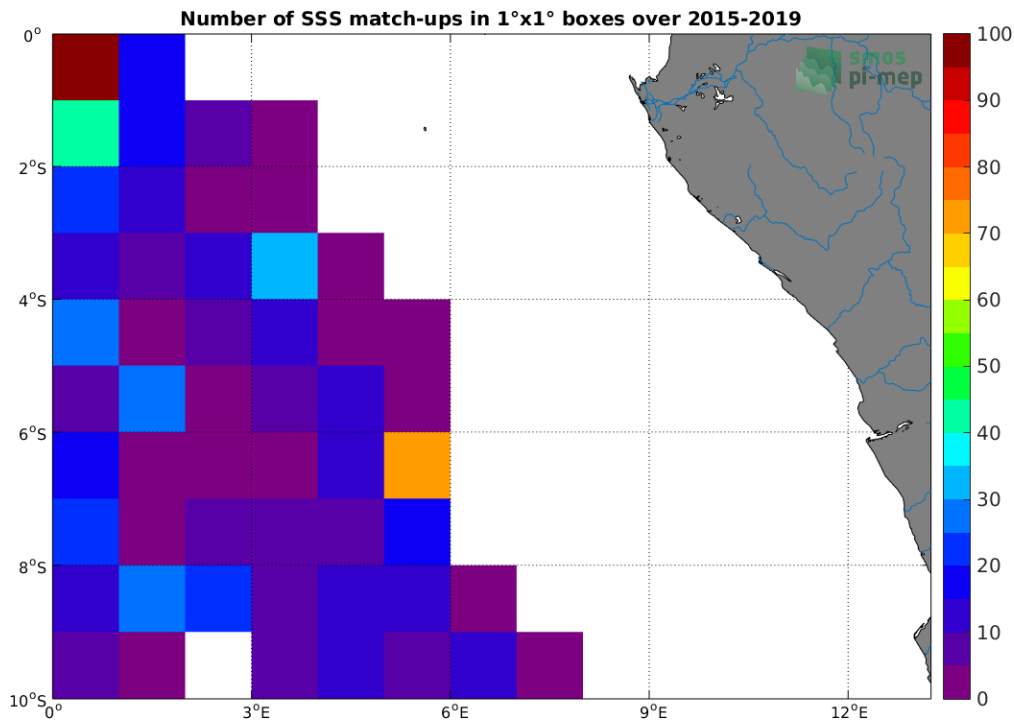
Figure 4: Number of SSS match-ups between Argo SSS and the SMAP-L3-RSS-V3-8DAY-RUNNING-70KM SSS product for the Congo river plume Pi-MEP region over 1°x1° boxes and for the full satellite product period.

2.5.5 Histograms of the spatial and temporal lags of the match-ups pairs

(a)

(b)
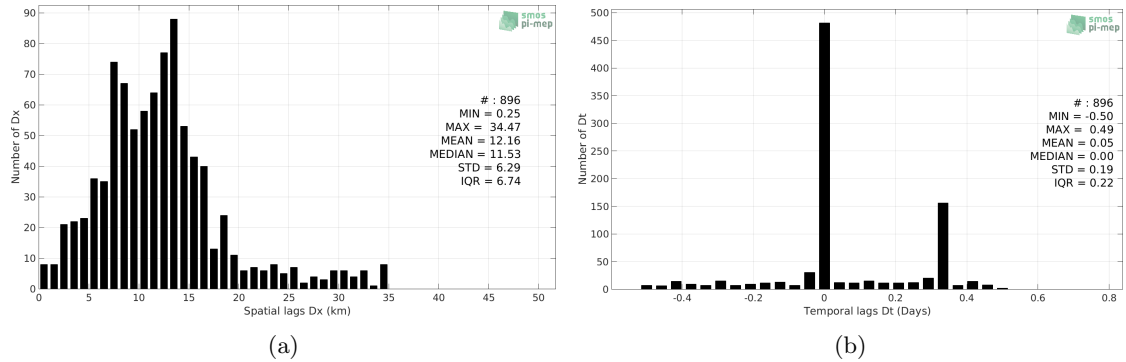
Figure 5: Histograms of the spatial (a) and temporal (b) lags between the time of the Argo measurements and the date of the corresponding SMAP-L3-RSS-V3-8DAY-RUNNING-70KM SSS product.

3 MDB file Analyses

3.1 Spatial Maps of the Temporal mean and Std of in situ and satellite SSS and of the difference (ΔSSS)

In Figure 6, we show maps of temporal mean (left) and standard deviation (right) of the SMAP-L3-RSS-V3-8DAY-RUNNING-70KM satellite SSS product (top) and of the Argo in situ dataset at the collected Pi-MEP match-up pairs. The temporal mean and std are gridded over the full satellite product period and over spatial boxes of size 1°x1°.

At the bottom of Figure 6, the temporal mean (left) and standard deviation (right) of the differences between the satellite SSS product and in situ data found at match-up pairs, namely ΔSSS(Satellite -Argo), is also gridded over the full satellite product period and over spatial boxes of size 1°x1°.

(a) MEAN(Satellite SSS)

(b) Std(Satellite SSS)

(c) MEAN(Argo SSS)

(d) Std(Argo SSS)

(e) MEAN(ΔSSS) (Satellite - Argo)

(f) Std(ΔSSS) (Satellite - Argo)

Figure 6: Temporal mean (left) and Std (right) of SSS from SMAP-L3-RSS-V3-8DAY-RUNNING-70KM (top), Argo (middle), and of ΔSSS (Satellite - Argo). Only match-up pairs are used to generate these maps.

3.2 Time series of the monthly averaged mean and Std of in situ and satellite SSS and of the (ΔSSS)

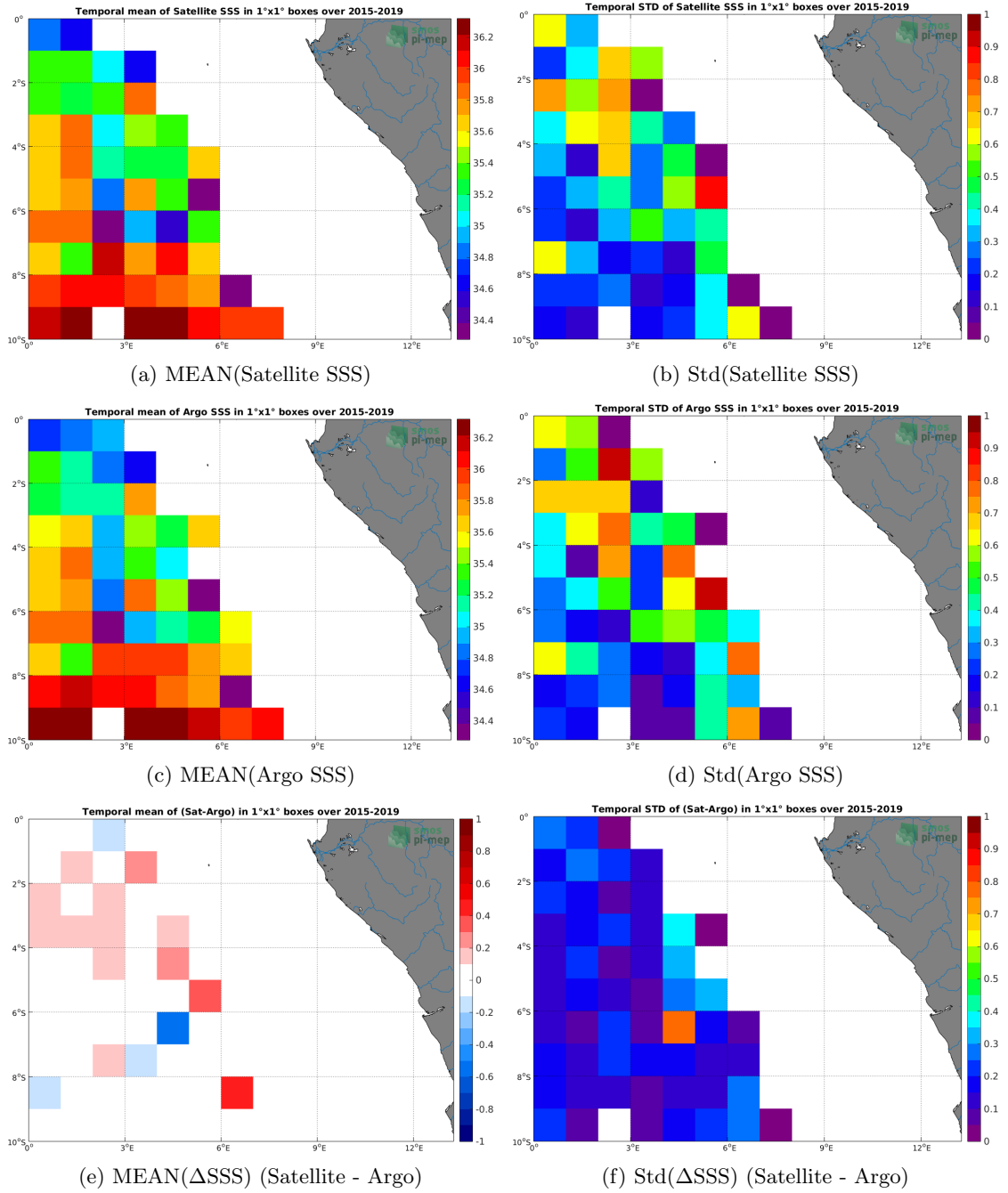In the top panel of Figure 7, we show the time series of the monthly averaged SSS estimated over the full Congo river plume Pi-MEP region for both SMAP-L3-RSS-V3-8DAY-RUNNING-70KM satellite SSS product (in black) and the Argo in situ dataset (in blue) at the collected Pi-MEP match-up pairs.

In the middle panel of Figure 7, we show the time series of the monthly averaged ΔSSS (Satellite - Argo) for the collected Pi-MEP match-up pairs and estimated over the full Congo river plume Pi-MEP region.

In the bottom panel of Figure 7, we show the time series of the monthly averaged standard deviation of the ΔSSS (Satellite - Argo) for the collected Pi-MEP match-up pairs and estimated over the full Congo river plume Pi-MEP region.
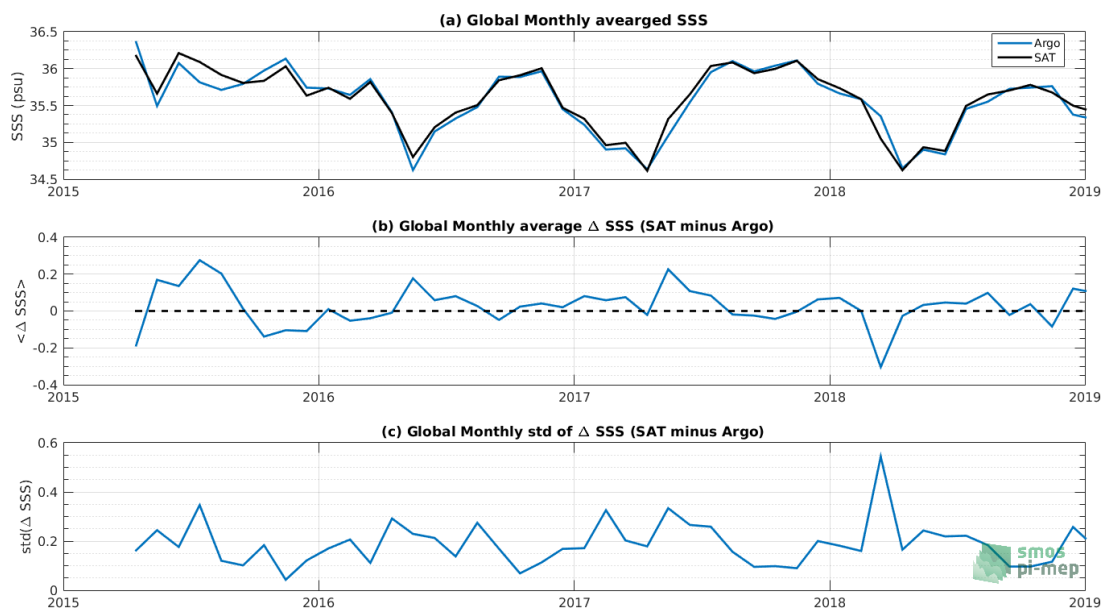
Figure 7: Time series of the monthly averaged mean SSS (top), mean ΔSSS (Satellite - Argo) and Std of ΔSSS (Satellite - Argo) over the Congo river plume Pi-MEP region considering all match-ups collected by the Pi-MEP platform.

3.3 Zonally-averaged Time-mean and temporal Std of in situ and satellite SSS and of the ΔSSS

In Figure 8 left panel, we show the zonally averaged time-mean SSS estimated at the collected Pi-MEP match-up pairs for both SMAP-L3-RSS-V3-8DAY-RUNNING-70KM satellite SSS product (in black) and the Argo in situ dataset (in blue). The time mean is evaluated over the full satellite SSS product period.

In the right panel of Figure 8, we show the zonally averaged time-mean ΔSSS (Satellite - Argo) for all the collected Pi-MEP match-up pairs estimated over the full satellite product period.

23
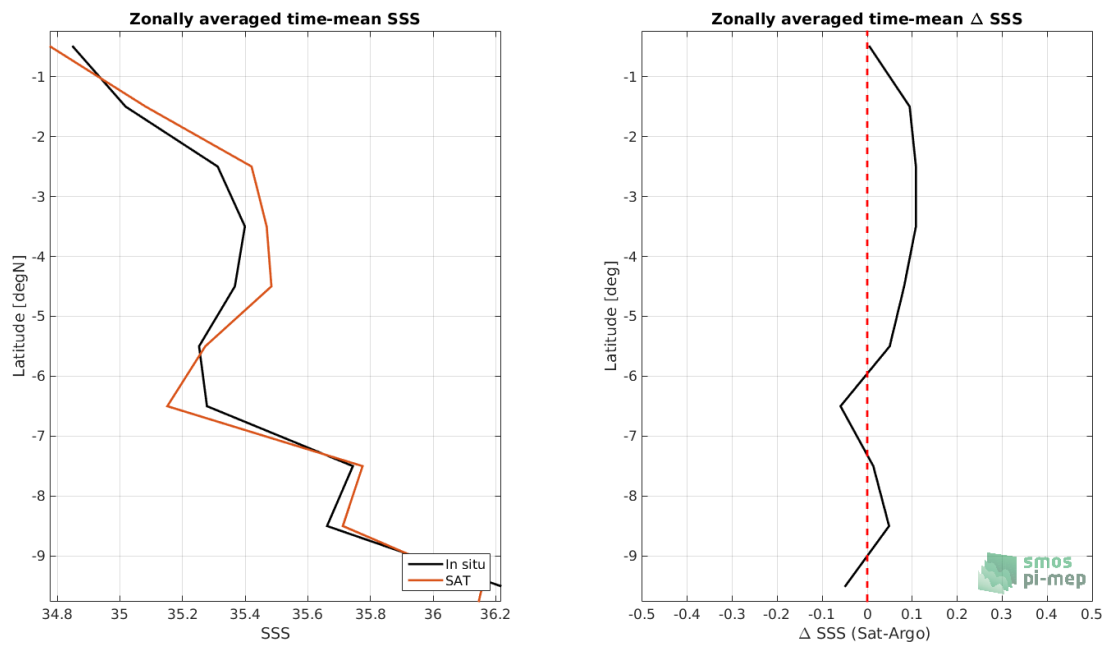
Figure 8: Left panel: Zonally averaged time mean SSS from SMAP-L3-RSS-V3-8DAY-RUNNING-70KM (black) and from Argo (blue). Right panel: zonally averaged time-mean ΔSSS (Satellite - Argo) for all the collected Pi-MEP match-up pairs estimated over the full satellite product period.

3.4 Scatterplots of satellite vs in situ SSS by latitudinal bands

(a) $0° \leq |\text{LAT}| \leq 80°$

(b) $0° \leq |\text{LAT}| \leq 20°$

(c) $20° \leq |\text{LAT}| \leq 40°$

(d) $40° \leq |\text{LAT}| \leq 60°$
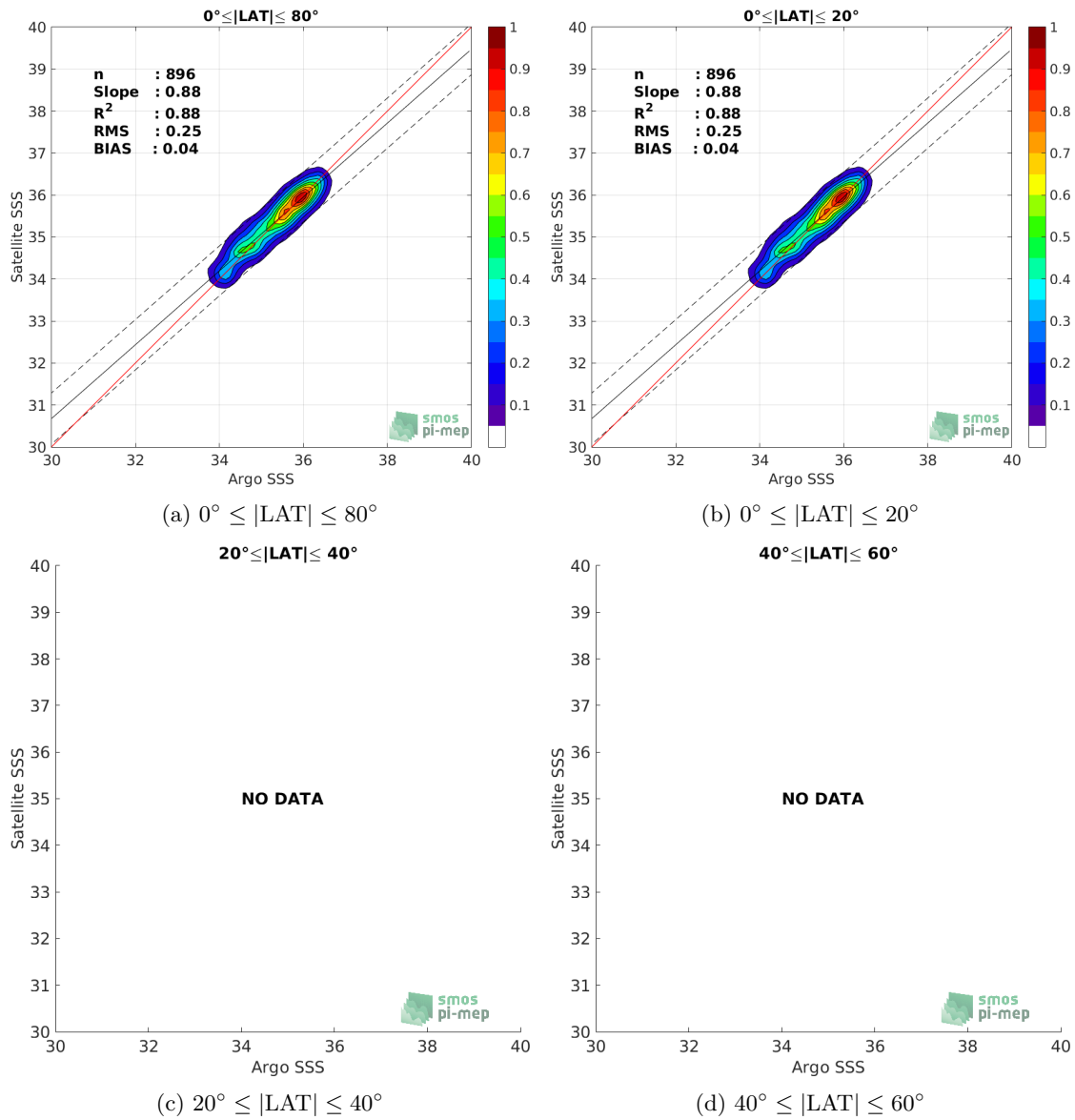
Figure 9: Contour maps of the concentration of SMAP-L3-RSS-V3-8DAY-RUNNING-70KM SSS (y-axis) versus Argo SSS (x-axis) at match-up pairs for different latitude bands. For each plot, the red line shows x=y. The black thin and dashed lines indicate a linear fit through the data cloud and the $\pm 95\%$ confidence levels, respectively. The number match-up pairs n, the slope and R^2 coefficient of the linear fit, the root mean square (RMS) and the mean bias between satellite and in situ data are indicated for each latitude band in each plots.

3.5 Time series of the monthly averaged mean and Std of the ΔSSS sorted by latitudinal bands

(a) $0° \leq |\text{LAT}| \leq 80°$

(b) $0° \leq |\text{LAT}| \leq 20°$

(c) $20° \leq |\text{LAT}| \leq 40°$

(d) $40° \leq |\text{LAT}| \leq 60°$
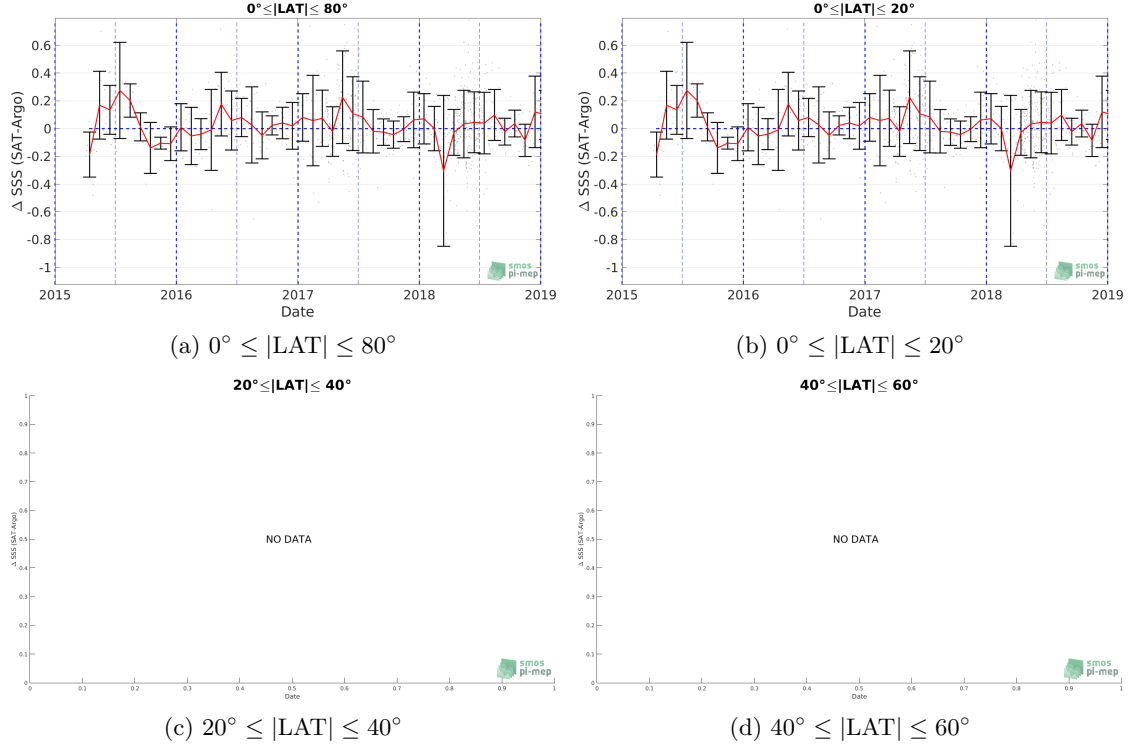
Figure 10: Monthly-average mean (red curves) ΔSSS (Satellite - Argo) and ±1 Std (black vertical thick bars) as function of time for all the collected Pi-MEP match-up pairs estimated over the Congo river plume Pi-MEP region and for the full satellite product period are shown for different latitude bands: (a) Latitude band 80°S-80°N, (b) latitude band 20°S-20°N, (c) Mid Latitude bands 40°S-20°S and 20°N-40°N and (d) Latitude bands 60°S-40°S and 40°N-60°N.

3.6 ΔSSS sorted as function of geophysical parameters

In Figure 11, we classify the match-up differences ΔSSS (Satellite - in situ) between SMAP-L3-RSS-V3-8DAY-RUNNING-70KM and Argo SSS as function of the geophysical conditions at match-up points. The mean and std of ΔSSS (Satellite - Argo) is thus evaluated as function of the

- in situ SSS values per bins of width 0.2,

- in situ SST values per bins of width 1°C,

- ASCAT daily wind values per bins of width 1 m/s,

- CMORPH 3-hourly rain rates per bins of width 1 mm/h, and,

- distance to coasts per bins of width 50 km.

26

(a) Argo SSS

(b) Argo SST

(c) ASCAT Wind Speed

(d) CMORPH Rain rate

(e) Distance to coast
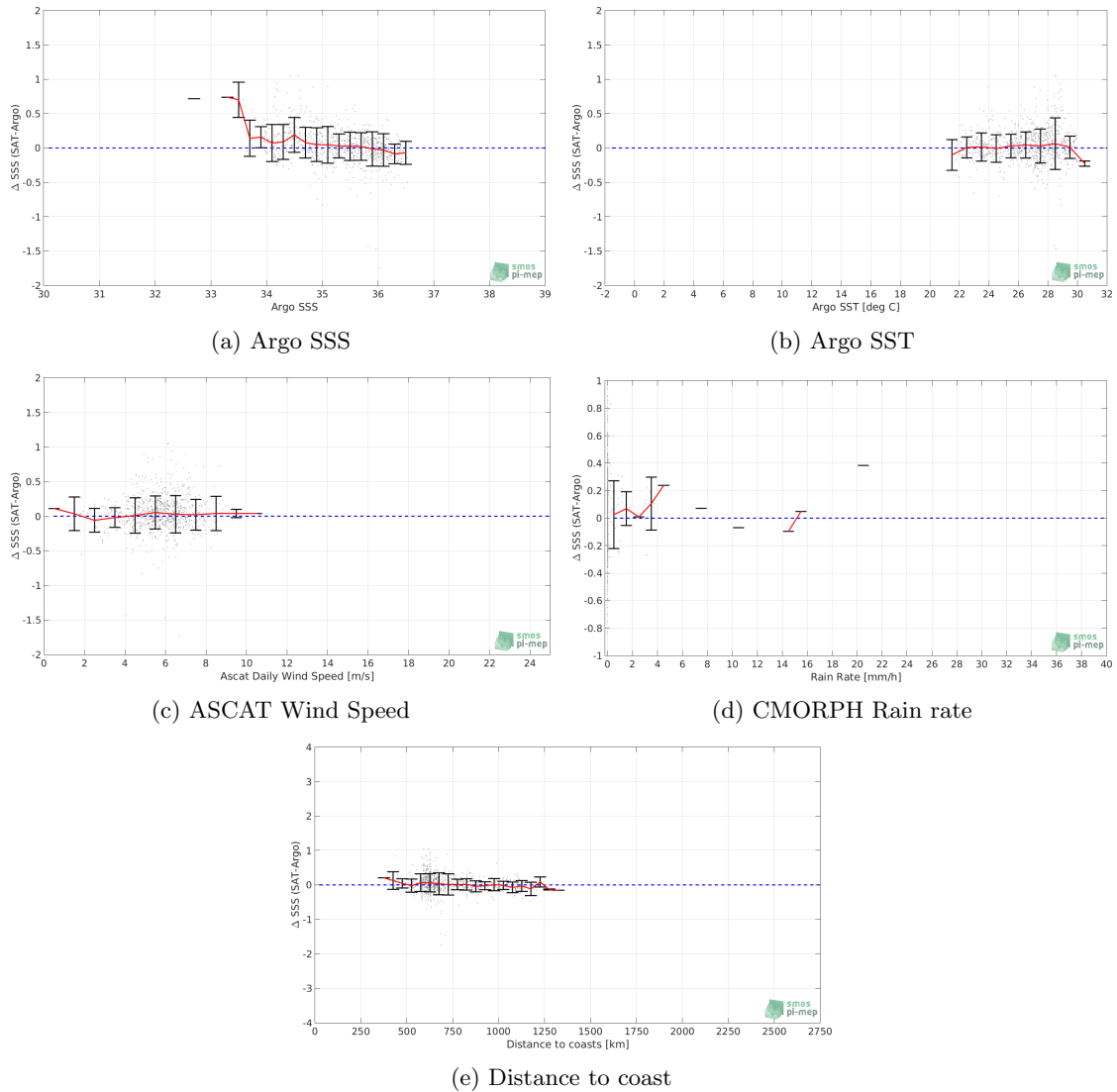
Figure 11: ΔSSS (Satellite - Argo) sorted as function of Argo SSS values a), Argo SST b), ASCAT Wind speed c), CMORPH rain rate d) and distance to coast (e). In all plots the mean and Std of ΔSSS for each bin is indicated by the red curves and black vertical thick bars (±1 Std)

3.7   ΔSSS maps and statistics for different geophysical conditions

In Figures 12 and 13, we focus on sub-datasets of the match-up differences ΔSSS (Satellite - in situ) between SMAP-L3-RSS-V3-8DAY-RUNNING-70KM and Argo for the following specific geophysical conditions:

- **C1**:if the local value at in situ location of estimated rain rate is zero, mean daily wind is in the range [3, 12] m/s, the SST is > 5°C and distance to coast is > 800 km.

- **C2**:if the local value at in situ location of estimated rain rate is zero, mean daily wind is in the range [3, 12] m/s.

- **C3**:if the local value at in situ location of estimated rain rate is high (ie. > 1 mm/h) and mean daily wind is low (ie. < 4 m/s).

- **C4**:if the mixed layer is shallow with depth <20m.

- **C5**:if the in situ data is located where the climatological SSS standard deviation is low (ie. above < 0.2).

- **C6**:if the in situ data is located where the climatological SSS standard deviation is high (ie. above > 0.2).

For each of these conditions, the temporal mean (gridded over spatial boxes of size 1°x1°) and the histogram of the difference ΔSSS (Satellite - in situ) are presented.

(a) RR=0 mm/h, 3< U_{10} <12 m/s, SST>5°C, distance to coast > 800 km

(b) RR=0 mm/h, 3< U_{10} <12 m/s

(c) RR>1mm/h and U_{10} <4m/s

(d) MLD<20m

(e) WOA2013 SSS Std<0.2

(f) WOA2013 SSS Std>0.2
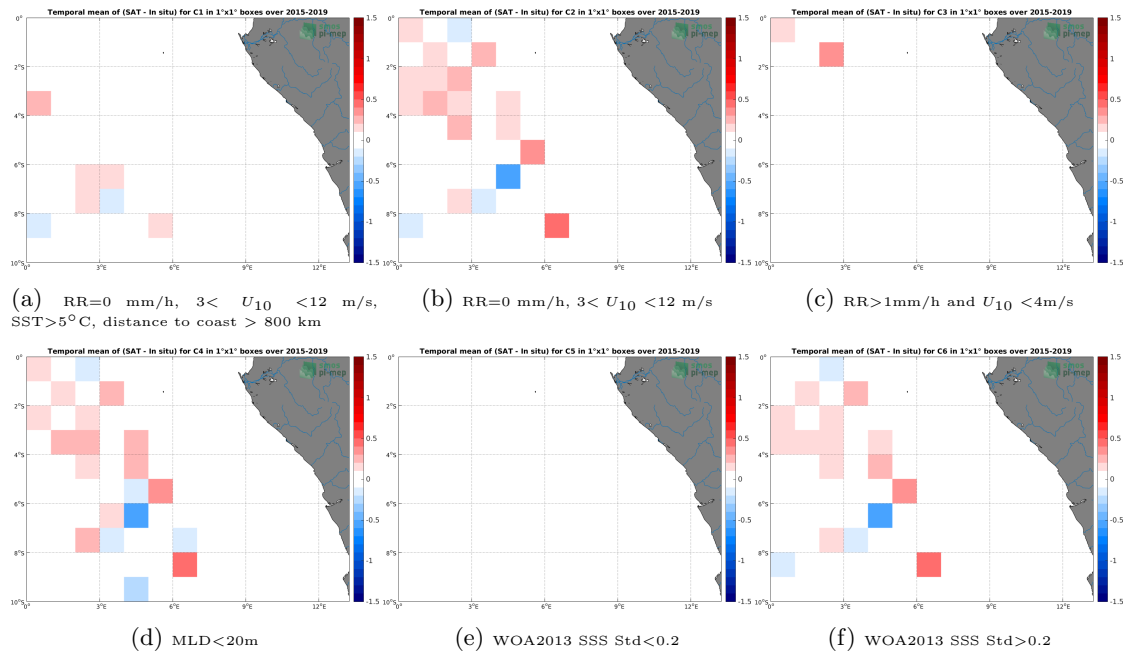
Figure 12: Temporal mean gridded over spatial boxes of size 1°x1° of ΔSSS (SMAP-L3-RSS-V3-8DAY-RUNNING-70KM - Argo) for 6 different subdatasets corresponding to:RR=0 mm/h, 3< U_{10} <12 m/s, SST>5°C, distance to coast > 800 km (a), RR=0 mm/h, 3< U_{10} <12 m/s (b), RR>1mm/h and U_{10} <4m/s (c),MLD<20m (d),WOA2013 SSS Std<0.2 (e),WOA2013 SSS Std>0.2 (f).

(a) RR=0 mm/h, 3< U_{10} <12 m/s, SST>5°C, distance to coast > 800 km

(b) RR=0 mm/h, 3< U_{10} <12 m/s

(c) RR>1mm/h and U_{10} <4m/s

(d) MLD<20m

(e) WOA2013 SSS Std<0.2

(f) WOA2013 SSS Std>0.2
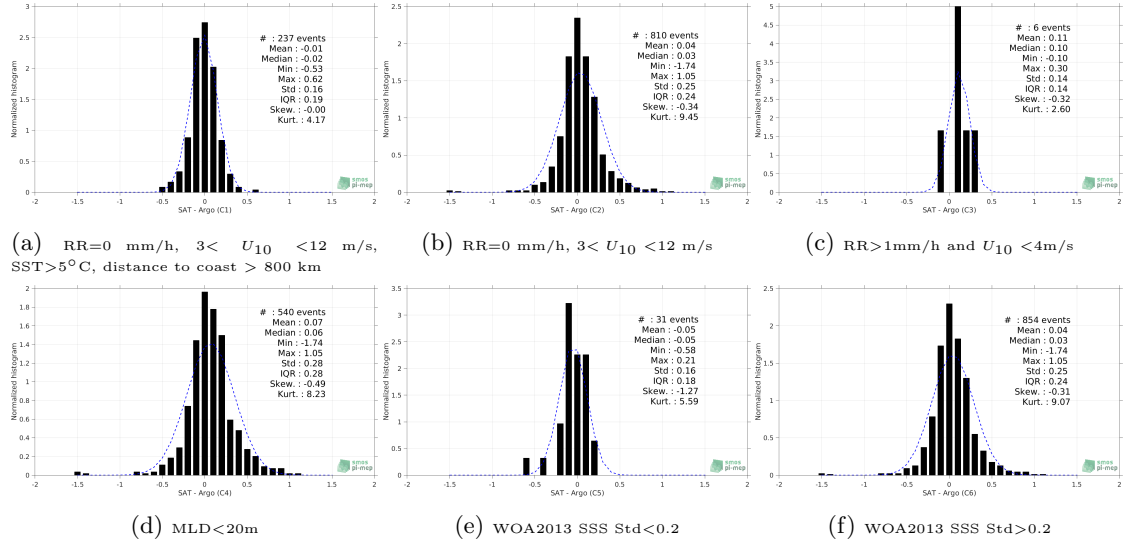
Figure 13: Normalized histogram of ΔSSS (SMAP-L3-RSS-V3-8DAY-RUNNING-70KM - Argo) for 6 different subdatasets corresponding to: RR=0 mm/h, 3< U_{10} <12 m/s, SST>5°C, distance to coast > 800 km (a), RR=0 mm/h, 3< U_{10} <12 m/s (b), RR>1mm/h and U_{10} <4m/s (c), MLD<20m (d), WOA2013 SSS Std<0.2 (e), WOA2013 SSS Std>0.2 (f).

4   Summary

Table 1 shows the mean, median, standard deviation (Std), root mean square (RMS), interquartile range (IQR), correlation coefficient (r^2) and robust standard deviation (Std*) of the match-up differences ΔSSS (Satellite - in situ) between SMAP-L3-RSS-V3-8DAY-RUNNING-70KM and Argo derived over the Congo river plume Pi-MEP region and for the full satellite product period and for the following conditions:

- all: All the match-up pairs satellite/in situ SSS are used to derive the statistics

- C1: only pairs where RR=0 mm/h, 3< U_{10} <12 m/s, SST>5°C, distance to coast > 800 km

- C2: only pairs where RR=0 mm/h, 3< U_{10} <12 m/s

- C3: only pairs where RR>1mm/h and U_{10} <4m/s

- C4: only pairs where MLD<20m

- C5: only pairs where WOA2013 SSS Std<0.2

- C6: only pairs at WOA2013 SSS Std>0.2

- C7a: only pairs where distance to coast is < 150 km.

- C7b: only pairs where distance to coast is in the range [150, 800] km.

- C7c: only pairs where distance to coast is > 800 km.

- C8a: only pairs where in situ SST is < 5°C.

- C8b: only pairs where in situ SST is in the range [5, 15]°C.

- C8c: only pairs where in situ SST is > 15°C.

- C9a: only pairs where in situ SSS is < 33.

- C9b: only pairs where in situ SSS is in the range [33, 37].

- C9c: only pairs where in situ SSS is > 37.

Table 1: Statistics of ΔSSS (Satellite - Argo)

Condition	#	Median	Mean	Std	RMS	IQR	r^2	Std*
all	896	0.03	0.04	0.24	0.25	0.24	0.88	0.18
C1	237	-0.02	-0.01	0.16	0.16	0.19	0.86	0.14
C2	810	0.03	0.04	0.25	0.25	0.24	0.88	0.18
C3	6	0.10	0.11	0.14	0.17	0.14	0.96	0.12
C4	540	0.06	0.07	0.28	0.29	0.28	0.84	0.21
C5	31	-0.05	-0.05	0.16	0.16	0.18	0.67	0.12
C6	854	0.03	0.04	0.25	0.25	0.24	0.88	0.18
C7a	0	NaN	NaN	NaN	NaN	NaN	NaN	NaN
C7b	652	0.04	0.06	0.27	0.27	0.27	0.84	0.19
C7c	244	-0.02	-0.01	0.16	0.16	0.19	0.86	0.14
C8a	0	NaN	NaN	NaN	NaN	NaN	NaN	NaN
C8b	0	NaN	NaN	NaN	NaN	NaN	NaN	NaN
C8c	896	0.03	0.04	0.24	0.25	0.24	0.88	0.18
C9a	1	0.72	0.72	0.00	0.72	0.00	NaN	0.00
C9b	895	0.03	0.04	0.24	0.25	0.24	0.88	0.18
C9c	0	NaN	NaN	NaN	NaN	NaN	NaN	NaN

Table 2 presents statistics of ΔSSS (Satellite - Argo) as Table 1 but for Argo delayed mode only.

Table 2: Statistics of ΔSSS (Satellite - Argo) - Delayed mode

Condition	#	Median	Mean	Std	RMS	IQR	r^2	Std*
all	296	0.01	0.02	0.19	0.20	0.22	0.92	0.16
C1	147	-0.02	-0.02	0.15	0.16	0.20	0.89	0.14
C2	281	0.01	0.02	0.20	0.20	0.22	0.92	0.16
C3	2	-0.02	-0.02	0.11	0.08	0.08	1.00	0.11
C4	150	0.06	0.06	0.23	0.24	0.26	0.91	0.20
C5	23	-0.05	-0.05	0.15	0.16	0.15	0.76	0.11
C6	262	0.01	0.03	0.20	0.20	0.22	0.92	0.17
C7a	0	NaN	NaN	NaN	NaN	NaN	NaN	NaN
C7b	147	0.05	0.07	0.22	0.23	0.22	0.90	0.17
C7c	149	-0.02	-0.02	0.15	0.16	0.20	0.89	0.14
C8a	0	NaN	NaN	NaN	NaN	NaN	NaN	NaN
C8b	0	NaN	NaN	NaN	NaN	NaN	NaN	NaN
C8c	296	0.01	0.02	0.19	0.20	0.22	0.92	0.16
C9a	1	0.72	0.72	0.00	0.72	0.00	NaN	0.00
C9b	295	0.01	0.02	0.19	0.19	0.22	0.92	0.16
C9c	0	NaN	NaN	NaN	NaN	NaN	NaN	NaN

For the same conditions, Table 3 presents statistics of ΔSSS (Satellite - ISAS). Only ISAS SSS values with PCTVAR<80% are used to derive the statistics.

Table 3: Statistics of ΔSSS (Satellite - ISAS)

Condition	#	Median	Mean	Std	RMS	IQR	r^2	Std*
all	885	0.01	0.03	0.32	0.32	0.38	0.77	0.29
C1	233	-0.05	-0.03	0.27	0.27	0.29	0.58	0.22
C2	801	0.01	0.03	0.33	0.33	0.38	0.76	0.29
C3	6	0.13	0.07	0.32	0.30	0.44	0.76	0.34
C4	536	0.01	0.02	0.34	0.34	0.40	0.74	0.30
C5	31	-0.07	0.06	0.38	0.38	0.23	0.30	0.17
C6	843	0.02	0.03	0.32	0.32	0.39	0.76	0.29
C7a	0	NaN	NaN	NaN	NaN	NaN	NaN	NaN
C7b	645	0.03	0.05	0.34	0.34	0.42	0.72	0.30
C7c	240	-0.05	-0.03	0.27	0.27	0.28	0.58	0.21
C8a	0	NaN	NaN	NaN	NaN	NaN	NaN	NaN
C8b	0	NaN	NaN	NaN	NaN	NaN	NaN	NaN
C8c	885	0.01	0.03	0.32	0.32	0.38	0.77	0.29
C9a	1	-0.68	-0.68	0.00	0.68	0.00	NaN	0.00
C9b	884	0.01	0.03	0.32	0.32	0.38	0.77	0.29
C9c	0	NaN	NaN	NaN	NaN	NaN	NaN	NaN

Numerical values can be downloaded as csv files for Table 1, Table 2 and Table 3.

References

Argo. Argo float data and metadata from Global Data Assembly Centre (Argo GDAC), 2000. doi: 10.17882/42182.

Abderrahim Bentamy and Denis Croize Fillon. Gridded surface wind fields from Metop/ASCAT measurements. *Int. J. Remote Sens.*, 33(6):1729–1754, March 2012. ISSN 1366-5901. doi: 10.1080/01431161.2011.600348.

Abderrahim Bentamy, Semyon A. Grodsky, James A. Carton, Denis Croizé-Fillon, and Bertrand Chapron. Matching ASCAT and QuikSCAT winds. *J. Geophys. Res.*, 117(C2), February 2012. ISSN 0148-0227. doi: 10.1029/2011JC007479. C02011.

Jaqueline Boutin, Y. Chao, W. E. Asher, T. Delcroix, R. Drucker, K. Drushka, N. Kolodziejczyk, T. Lee, N. Reul, G. Reverdin, J. Schanze, A. Soloviev, L. Yu, J. Anderson, L. Brucker, E. Dinnat, A. S. Garcia, W. L. Jones, C. Maes, T. Meissner, W. Tang, N. Vinogradova, and B. Ward. Satellite and In Situ Salinity: Understanding Near-Surface Stratification and Sub-footprint Variability. *Bull. Am. Meterol. Soc.*, 97(8):1391–1407, 2016. ISSN 1520-0477. doi: 10.1175/bams-d-15-00032.1.

Clément de Boyer Montégut, Gurvan Madec, A. S. Fischer, A. Lazar, and D. Ludicone. Mixed layer depth over the global ocean: An examination of profile data and a profile-based climatology. *J. Geophys. Res.*, 109(C12):C12003, December 2004. ISSN 0148-0227. doi: 10.1029/2004jc002378.

Clément de Boyer Montégut, Juliette Mignot, Alban Lazar, and Sophie Cravatte. Control of salinity on the mixed layer depth in the world ocean: 1. General description. *J. Geophys. Res.*, 112(C6):C06011, June 2007. ISSN 0148-0227. doi: 10.1029/2006jc003953.

Ralph R. Ferraro. SSM/I derived global rainfall estimates for climatological applications. *J. Geophys. Res.*, 1021:16715–16736, 07 1997. doi: 10.1029/97JD01210.

Ralph R. Ferraro, Fuzhong Weng, Norman C. Grody, and Limin Zhao. Precipitation characteristics over land from the NOAA-15 AMSU sensor. *Geophys. Res. Lett.*, 27(17):2669–2672, 2000. doi: 10.1029/2000GL011665.

Fabienne Gaillard, E. Autret, V. Thierry, P. Galaup, C. Coatanoan, and T. Loubrieu. Quality Control of Large Argo Datasets. *J. Atmos. Oceanic Technol.*, 26(2):337–351, 2012/10/10 2009. doi: 10.1175/2008JTECHO552.1.

Fabienne Gaillard, Thierry Reynaud, Virginie Thierry, Nicolas Kolodziejczyk, and Karina von Schuckmann. In Situ-Based Reanalysis of the Global Ocean Temperature and Salinity with ISAS: Variability of the Heat Content and Steric Height. *J. Clim.*, 29(4):1305–1323, February 2016. ISSN 1520-0442. doi: 10.1175/jcli-d-15-0028.1.

Robert J. Joyce, John E. Janowiak, Phillip A. Arkin, and Pingping Xie. CMORPH: A Method that Produces Global Precipitation Estimates from Passive Microwave and Infrared Data at High Spatial and Temporal Resolution. *J. Hydrometeorol.*, 5(3):487–503, June 2004. ISSN 1525-7541. doi: 10.1175/1525-7541(2004)005⟨0487:camtpg⟩2.0.co;2.

Nicolas Kolodziejczyk, Gilles Reverdin, and Alban Lazar. Interannual Variability of the Mixed Layer Winter Convection and Spice Injection in the Eastern Subtropical North Atlantic. *J. Phys. Oceanogr.*, 45(2):504–525, Feb 2015. ISSN 1520-0485. doi: 10.1175/jpo-d-14-0042.1.

Christian Kummerow, Y. Hong, W. S. Olson, S. Yang, R. F. Adler, J. McCollum, R. Ferraro, G. Petty, D-B. Shin, and T. T. Wilheit. The Evolution of the Goddard Profiling Algorithm (GPROF) for Rainfall Estimation from Passive Microwave Sensors. *J. Appl. Meteorol.*, 40(11): 1801–1820, 2001. doi: 10.1175/1520-0450(2001)040⟨1801:TEOTGP⟩2.0.CO;2.